JOURNAL OF BACTERIOLOGY, Nov. 2007, p. 8120–8129 Vol. 189, No. 22
0021-9193/07/$08.00+0 doi:10.1128/JB.01247-07

Phosphate-Controlled Regulator for the Biosynthesis of the Dalbavancin Precursor A40926▽†

Rosa Alduina,[1]* Luca Lo Piccolo,[1] Davide D'Alia,[1]‡ Clelia Ferraro,[1] Nina Gunnarsson,[2]§ Stefano Donadio,[3] and Anna Maria Puglia[1]

University of Palermo, Dipartimento di Biologia Cellulare e dello Sviluppo, Viale delle Scienze, Parco d'Orleans II, 90128 Palermo, Italy[1]; Biocentrum-DTU, Center for Microbial Biotechnology, Building 223, Soltofts plads, 2800 Lyngby, Denmark[2]; and KtedoGen, Malnate, Italy[3]

Received 2 August 2007/Accepted 5 September 2007

The actinomycete *Nonomuraea* sp. strain ATCC 39727 produces the glycopeptide A40926, the precursor of the novel antibiotic dalbavancin. Previous studies have shown that phosphate limitation results in enhanced A40926 production. The A40926 biosynthetic gene (*dbv*) cluster, which consists of 37 genes, encodes two putative regulators, Dbv3 and Dbv4, as well as the response regulator (Dbv6) and the sensor-kinase (Dbv22) of a putative two-component system. Reverse transcription-PCR (RT-PCR) and real-time RT-PCR analysis revealed that the *dbv14-dbv8* and the *dbv30-dbv35* operons, as well as *dbv4*, were negatively influenced by phosphate. Dbv4 shows a putative helix-turn-helix DNA-binding motif and shares sequence similarity with StrR, the transcriptional activator of streptomycin biosynthesis in *Streptomyces griseus*. Dbv4 was expressed in *Escherichia coli* as an N-terminal His_6-tagged protein. The purified protein bound the *dbv14* and *dbv30* upstream regions but not the region preceding *dbv4*. Bbr, a Dbv4 ortholog from the gene cluster for the synthesis of the glycopeptide balhimycin, also bound to the *dbv14* and *dbv30* upstream regions, while Dbv4 bound appropriate regions from the balhimycin cluster. Our results provide new insights into the regulation of glycopeptide antibiotics, indicating that the phosphate-controlled regulator Dbv4 governs two key steps in A40926 biosynthesis: the biosynthesis of the nonproteinogenic amino acid 3,5-dihydroxyphenylglycine and critical tailoring reactions on the heptapeptide backbone.

The filamentous actinomycete *Nonomuraea* sp. strain ATCC 39727 produces the glycopeptide antibiotic A40926 (11), which belongs to the teicoplanin family and is the precursor of dalbavancin, a promising antibiotic for treatment of infections by multiresistant gram-positive bacteria (4, 37). In recent years, considerable progress has been made in understanding glycopeptide biosynthesis. Chemically, this family of glycopeptide antibiotics consists of a heptapeptide core constituted by proteinogenic and nonproteinogenic amino acids such as 3,5-dihydroxyphenylglycine (DPG) and 4-hydroxyphenylglycine (HPG). The heptapeptides are assembled by nonribosomal peptide synthetases (NRPS) and then extensively modified by oxidative cross-linking of the electron-rich aromatic side chains (14, 40). The cross-links make the peptide scaffold rigid, creating the binding pocket for the drug target, the terminal D-Ala–D-Ala moiety of peptidoglycan (45). Further tailoring steps may include halogenation, glycosylation, methylation, acylation, and sulfation.

The *dbv* gene cluster for the biosynthesis of A40926 (33, 35) includes 37 open reading frames participating in antibiotic biosynthesis, regulation, resistance, and export (Fig. 1A). Specifically, the cluster encodes the putative regulators Dbv3 (LuxR-like) and Dbv4 (StrR-like), as well as the putative response regulator Dbv6 and the sensor-kinase Dbv22, that may be part of a two-component system. Sequence information is also available for five other gene clusters devoted to glycopeptides, namely, chloroeremomycin (*cep*) (44), balhimycin (*bal*) (24, 27), complestatin (*com*) (6), A47934 (*sta*) (26), and teicoplanin (*tcp*) (18, 34). All clusters contain an *strR*-like regulator. StrR is a well-studied pathway-specific transcriptional regulator that activates the expression of streptomycin biosynthetic genes in *Streptomyces griseus* and *Streptomyces glaucescens* (28). Other StrR-like regulators have been characterized, such as NovG from the *Streptomyces caeruleus* novobiocin cluster (10), CloG from the *Streptomyces roseochromogenes* clorobiocin cluster (10), and KasT from the *Streptomyces kasugaensis* kasugamycin cluster (13).

Recently, the production of A40926 was found to be influenced by phosphate (12, 42). In particular, Gunnarsson et al. (12) found that low initial phosphate concentrations were beneficial for A40926 production and that the onset of production was not governed by the residual phosphate concentration, although its level strongly influenced production rates and final titers. These results were independently confirmed by Technikova-Dobrova et al. (42). The molecular bases for phosphate regulation of A40926 production have not yet been studied. We demonstrate here that expression of the regulatory gene *dbv4* is phosphate controlled. Furthermore, Dbv4 specifically controls the expression of two *dbv* operons, one encoding the

* Corresponding author. Mailing address: Dipartimento di Biologia Cellulare e dello Sviluppo, Università degli Studi di Palermo, Viale delle Scienze, Parco d'Orleans II, 90128 Palermo, Italy. Phone: 39 091 6577306. Fax: 39 091 6577347. E-mail: valduina@unipa.it.

† Supplemental material for this article may be found at http://jb.asm.org/.

‡ Present address: Groningen Biomolecular Sciences and Biotechnology Institute (GBB), University of Groningen, Kerklaan 30, 9751 NN Haren, The Netherlands.

§ Present address: Fluxome Sciences A/S, Diplomvej 378, 2800 Lyngby, Denmark.

▽ Published ahead of print on 14 September 2007.

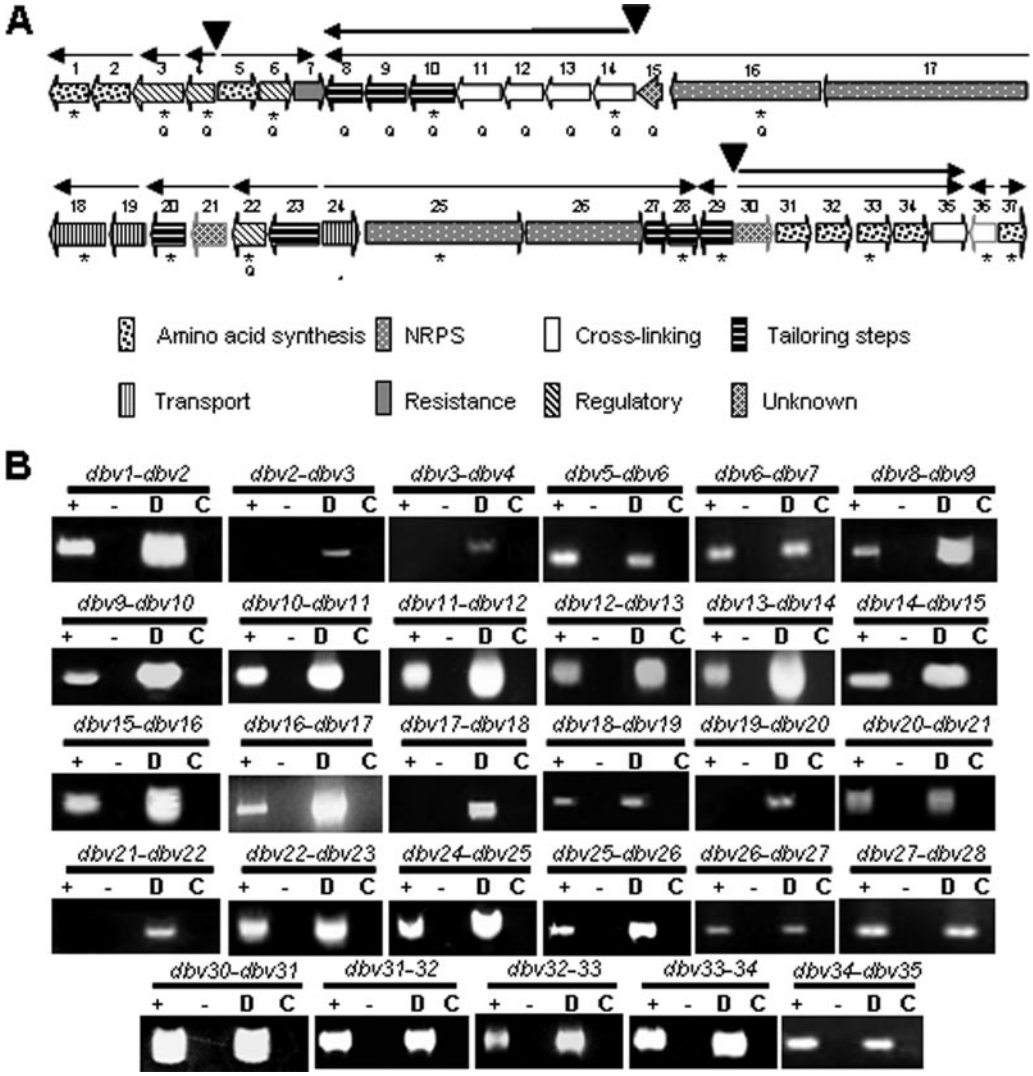

FIG. 1. Organization of the 71-kb *dbv* cluster and transcriptional map. (A) Genomic organization of the 71-kb *dbv* cluster. The thin arrows represent the experimentally determined transcriptional units; the thick arrows indicate the Dbv4-controlled *dbv14-dbv8* and *dbv30-dbv35* operons; triangles denote DNA fragments used in gel retardation experiments; asterisks and the symbol "Q" indicate genes targeted by RT-PCR and quantitative RT-PCR, respectively. *dbv* genes are grouped by category as indicated (33, 35). (B) RT-PCR analysis of intergenic regions. Total RNA, extracted after 47 h of growth under LowP conditions, was used as a template in the presence (+) or in the absence (−) of reverse transcriptase. Lanes D and C represent positive (DNA) and negative (water) controls, respectively.

proteins involved in synthesizing DPG and the other devoted to cross-linking, halogenation, glycosylation, and acylation of the heptapeptide scaffold. These studies provide a platform for rational manipulation of the industrially important producer strain to increase A40926 production.

MATERIALS AND METHODS

Bacterial strains and plasmid construction. *Nonomuraea* sp. strain ATCC 39727 (11), *Streptomyces lividans* ZX7 (15), and *Escherichia coli* DH5α and BL21 (Invitrogen) were used in this study. Plasmids pGEM-T (Promega), pIJ486 (15), and pRSETB (Invitrogen) were used for cloning PCR products, promoter probe studies, and protein expression, respectively.

The *dbv14* promoter region (from −141 bp to +30 bp of the *dbv14* coding region) was PCR amplified, using *Nonomuraea* chromosomal DNA as a template and the primer pair *pdbv14*For-*pdbv14*Rev (see Table S1 in the supplemental material), and cloned into pGEM-T, yielding pGEM-*pdbv*14. The insert was then excised with EcoRI and cloned into the EcoRI site of pIJ486. The resulting plasmid, pIJ486-*pdbv*14, was used to transform *S. lividans* ZX7 protoplasts (15). Transformants were tested on MM plates (15) supplemented with neomycin or kanamycin. *dbv4* was amplified by PCR with *Nonomuraea* chromosomal DNA as a template and the primers 5′-AAAATGATCAGGTGGACCCGACGGGAGT T-3′ and 5′-AAAAAAGCTTTCATCCAGCGGCCAGATC-3′ (underlines indicate the BclI and HindIII sites, respectively). The amplified fragment was digested with BclI plus HindIII and ligated into the BamHI and HindIII sites of pRSETB, yielding pRSET-Dbv4, which was introduced into BL21(DE3)pLysS cells. Plasmid pRSET-Dbv4 expresses the entire Dbv4 protein with a His_6 tag at its N terminus under the control of the T7 promoter and the *lac* operator. Fidelity of PCR amplifications was confirmed by DNA sequencing.

Total RNA isolation, RT-PCR analysis, and real-time RT-PCR. *Nonomuraea* was cultivated in 1-liter controlled bioreactors with cultivation conditions and growth medium compositions as described previously (12). Samples for biomass dry weight, A40926, glucose, and phosphate in the medium were withdrawn during the time course of the cultivations and analyzed as described previously (12). Aliquots (5 ml; containing about 20 mg of dried cell weight) were filtered under vacuum on Supor-450 filters (Pall Corp.), and the biomass was collected from the filter and immediately frozen in liquid nitrogen. The cells were broken

by using 1 mg of lysozyme/ml in P-buffer (15) or by grinding in liquid nitrogen, and total RNA was isolated by using the RNeasy midi-kit (QIAGEN). DNase I (Roche) treatment was performed at 37°C for 1 h, and ethanol precipitation in the presence of 0.1 vol 3 M sodium acetate allowed recovery of the DNase-treated total RNA. After a washing step with 70% ethanol and air drying, the RNA pellet was resuspended in water. Reverse transcription-PCR (RT-PCR) was performed by using a Superscript One-Step RT-PCR kit (Invitrogen) with about 0.1 μg of total RNA as a template, primer pairs internal to *dbv* genes, and the conditions indicated by the supplier, routinely using 30 PCR cycles. Expression of the *Nonomuraea hrdB* gene was monitored by using primers kindly provided by Riham Shawky, University of Tubingen. Other primers are listed in Table S1 of the supplemental material. For each reaction, a negative control with *Taq* polymerase and without reverse transcriptase was included. To assess co-transcription, RT-PCR analysis was carried out on RNA extracted after 47 h of growth under low-phosphate (LowP) conditions using specific primer (see Table S1 in the supplemental material). Each pair was designed to amplify a fragment extending from 250 to 300 bp upstream of the stop codon of a gene to 250 to 300 bp downstream of the start codon of the following gene. PCRs were performed on fivefold-more-concentrated RNA samples using 40 cycles prior to exclude the presence of genomic DNA. The identities of the RT-PCR products were confirmed by sequencing.

Expression was analyzed quantitatively by real-time RT-PCR using the Applied Biosystems 7300 real-time PCR system (Applied Biosystems). A high-capacity cDNA archive kit (Applied Biosystems) was used, according to the manufacturer's instructions, to retrotranscribe 5 μg of total RNA, extracted after 42 and 60 h of growth from LowP and high-phosphate (HighP) cultures, in a final volume of 100 μl of water. Then, 3 μl of the cDNA was mixed with 10 μl of SYBR green PCR master mix (Applied Biosystem) and 10 pmol of each primer in a final volume of 20 μl. The PCR was performed under the following conditions: 2 min at 50°C and 10 min at 95°C, followed by 40 cycles of 15 s at 95°C and 1 min at 68°C. Eventually, a dissociation reaction was performed with the following conditions: a 1-min step with a temperature gradient increase of 1°C per step from 55 to 99°C. This last reaction allowed the melting curve of the PCR products and, consequently, their specificity to be determined. A negative control (distilled water) was included in all real-time PCR assays, and each experiment was performed in triplicate. The *hrdB*-like gene was used as an internal control to quantify the relative expression of target genes.

Mapping of the *dbv14* transcription start point. The 5′ end of the *dbv14* transcript was determined by using the 5′ RACE system (version 2.0; Invitrogen) according to the manufacturer's instructions. Briefly, RT was performed on 5 μg of total RNA, extracted after 47 h of growth, using 5 pmol of 5′-GGCGTCCA GGCAGTCC-3′ (located 368 bp upstream the *dbv14* traslational start codon) and 200 U of Superscript II reverse transcriptase in a final volume of 25 μl. After RNA digestion with RNase H and purification with the GlassMax DNA Isolation Spin Cartridges (Invitrogen), the cDNA was 3′ tailed with poly(dT). Subsequently, 5 μl of dT-tailed cDNA was used as a template in nested PCRs using the specific primers (5′-CGCCGTAGAGCAACCTGGAGC-3′; 206 bp upstream), 5′-CTCGGCGCCCAGCTCGGTCAT-3′; 105 bp upstream), and 5′-CCGGTC CCTCCAGTGCAGCTC-3′; 39 bp upstream) and the Abridged Anchor and Abridged Universal Anchor primers supplied with the kit. The resulting 100-bp PCR product was cloned into pGEM-T and sequenced.

Dbv4 expression. *E. coli* BL21(DE3) harboring pRSET-Dbv4 produced His_6-Dbv4 mostly in the insoluble fraction. After several trials, we eventually settled on the following conditions. *E. coli* cells were cultured overnight at 37°C in LB medium containing 25 μg of chloramphenicol/ml and 25 μg of ampicillin/ml, and 5 ml was transferred into 50 ml of fresh LB medium and cultured at 37°C until it achieved an optical density at 600 nm of about 1.0. Dbv4 expression was induced by adding 0.5 mM IPTG (isopropyl-β-D-thiogalactopyranoside). After 2 h, the cells were harvested by centrifugation and disrupted by sonication. Soluble fractions were separated by centrifugation, and proteins were purified by using Ni-NTA agarose (Invitrogen). Proteins were eluted with 250 mM imidazole, concentrated by Millipore columns, dialyzed against 12.5 mM Tris-HCl (pH 7.5)–10% glycerol–62.5 mM KCl–0.75 mM dithiothreitol (DTT), and stored in the same buffer at −80°C before use. The protein concentration was determined with the Bradford reagent (Bio-Rad). From 50 ml of cultures, about 0.5 to 1 mg of Dbv4 was obtained. Bbr (30) was kindly provided by Riham Shawky, University of Tubingen.

Preparation of *Nonomuraea* total proteins. *Nonomuraea* sp. ATCC 39727 was grown for 70 h at 30°C in 200 ml of Rare3 medium (33). The cells were then harvested by centrifugation, washed twice with crack buffer (10 mM Tris-HCl [pH 8.0], 0.5 mM EDTA, 0.3 mM DTT), resuspended in 5 ml of crack buffer, and disrupted by sonication. The cell debris was removed by centrifugation at 20,000 × *g* (20 min, 4°C), and the supernatant was stored at −80°C.

Gel mobility shift assay. The gel mobility shift assay was performed according to the method of Retzlaff and Distler (28). For the binding assay, approximately 0.2 μg of Dbv4 or Bbr was incubated for 10 min at 4°C in 20 μl of 12.5 mM Tris-HCl (pH 7.5), 10% glycerol, 62.5 mM KCl, 0.75 mM DTT, and 5 mM $MgCl_2$ containing 50 μg of poly(dI-dC)-poly(dI-dC) ml^{-1}. In experiments with *Nonomuraea* total proteins (200 μg), 100 μg of poly(dI-dC)-poly(dI-dC) ml^{-1} was used. After 15 min of incubation with 0.4 ng of ^{32}P-labeled DNA, complexes and free DNA were resolved on nondenaturing 5% polyacrylamide gels run in 0.5× Tris-borate-EDTA buffer at 150 V for approximately 2 h (29) and then equilibrated in 10% acetic acid, dried, and subjected to autoradiography. For testing the specificity of binding, unlabeled probe or competitor DNA fragments were added before incubation of the protein(s) and probe.

Preparation of labeled DNA fragments. DNA fragments of 352, 171, 351, 158, and 232 bp, containing the *dbv4*, *dbv14*, *dbv30*, *bbr*, and *oxyA* upstream regions, respectively, were prepared by PCR in the presence of [α-^{32}P]CTP, using the primers reported in Table S1 in the supplemental material. The 50-bp fragments 14A, 14B, 14C, and 14D were prepared by incubation of the corresponding oligonucleotides at 90°C for 10 min, followed by slow cooling to room temperature. The annealed products were recovered from nondenaturing 20% polyacrylamide gels by the crush-soak method (29) and labeled with T4 polynucleotide kinase (Invitrogen) according to the supplier's protocol.

RESULTS

Transcriptional organization of the *dbv* gene cluster. The genomic organization of the *dbv* cluster (Fig. 1A) suggests the presence of at least five polycistronic transcriptional units (*dbv4-dbv1*, *dbv5-dbv7*, *dbv23-dbv8*, *dbv24-dbv28*, and *dbv30-dbv35*) and three monocistronic units (*dbv29*, *dbv36*, and *dbv37*). To investigate the transcriptional organization of the *dbv* cluster, total RNA was used as a template for RT-PCR using selected primer pairs (see Table S1 in the supplemental material). When amplification products of expected size were obtained, they were authenticated by sequencing. RT-PCR analysis (Fig. 1B) indicated that, at least under the conditions used, the genes *dbv1-dbv2*, *dbv5-dbv7*, *dbv17* through *dbv8*, *dbv19-dbv18*, *dbv21-dbv20*, *dbv23-dbv22*, *dbv24* through *dbv28*, and *dbv30* through *dbv35* are cotranscribed, while *dbv3* and *dbv4* are transcribed as monocistronic units (Fig. 1A).

Expression of *dbv* genes under LowP and HighP concentrations. To study the influence of phosphate on *dbv* gene expression, *Nonomuraea* sp. strain ATCC 39727 was cultivated in a defined growth medium (12) containing either 4.2 or 2 mM phosphate (HighP and LowP conditions, respectively). As shown in Fig. 2, A40926 production started at 42 h and proceeded at an identical rate up to 47 h under both conditions. However, a significant increase in specific A40926 productivity was observed under LowP conditions, once the phosphate concentration went below 0.1 mM at 47 h. In contrast, the productivity under HighP conditions remained low, even when phosphate concentrations reached comparable low values (e.g., at 60 and 71 h).

Total RNA isolated before (at 28 and 35 h) and during A40926 production (at 42, 47, 60, and 71 h) was analyzed by RT-PCR. We concentrated on a subset of *dbv* genes, selecting them on the basis of function and transcriptional organization (see Fig. 1A for details). Thus, we analyzed the four putative regulatory genes (*dbv3*, *-4*, *-6*, and *-22*), four genes involved in the biosynthesis of DPG and HPG (*dbv1*, *-28*, *-33*, and *-37*), two NRPS genes (*dbv16* and *-25*), and the genes encoding a cross-linking oxygenase (*dbv14*), the halogenase (*dbv10*), an ABC transporter (*dbv18*), the mannosyltransferase (*dbv20*), the hexose oxidase (*dbv29*), and a type II thioesterase (*dbv36*).

The expression of the *Nonomuraea hrdB* gene, likely to en-

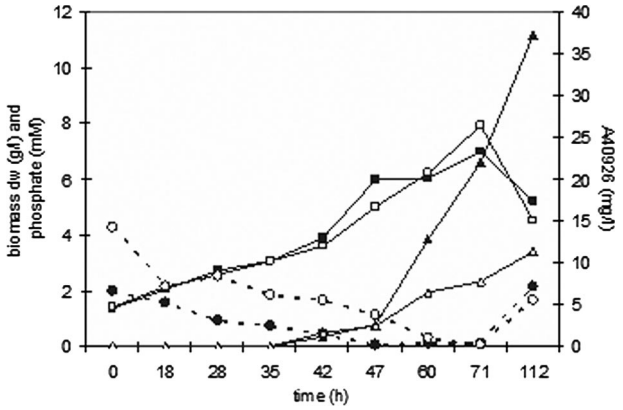

FIG. 2. A40926 production in batch fermentation. Growth (squares), phosphate concentration (circles), and A40926 production (triangles) were monitored with initial phosphate concentrations of 2 mM (LowP; closed symbols) and 4.2 mM (HighP; open symbols).

code a constitutive vegetative sigma factor, was monitored as a control. As shown in Fig. 3, *hrdB* transcripts were detected at similar levels in all of the samples tested. RT-PCR analysis revealed that most *dbv* genes analyzed (*dbv1*, *-3*, *-6*, *-16*, *-18*, *-20*, *-22*, *-25*, *-28*, *-29*, *-36*, and *-37*) were expressed at similar levels throughout growth under the two phosphate conditions (Fig. 3). However, *dbv4*, *dbv10*, *dbv14*, and *dbv33* were upregulated under phosphate depletion (Fig. 3).

To confirm these results, we analyzed the expression of 20 *dbv* genes by quantitative real-time RT-PCR. cDNA molecules were retrotranscribed from the total RNA extracted after 42 and 60 h of growth under both HighP and LowP conditions, with *hrdB* used as an internal control. The 60-h, HighP-sample was used to normalize expression levels. This analysis confirmed that *dbv4* and the genes of the *dbv30-dbv35* and *dbv14-dbv8* operons were negatively regulated by phosphate (Fig. 4).

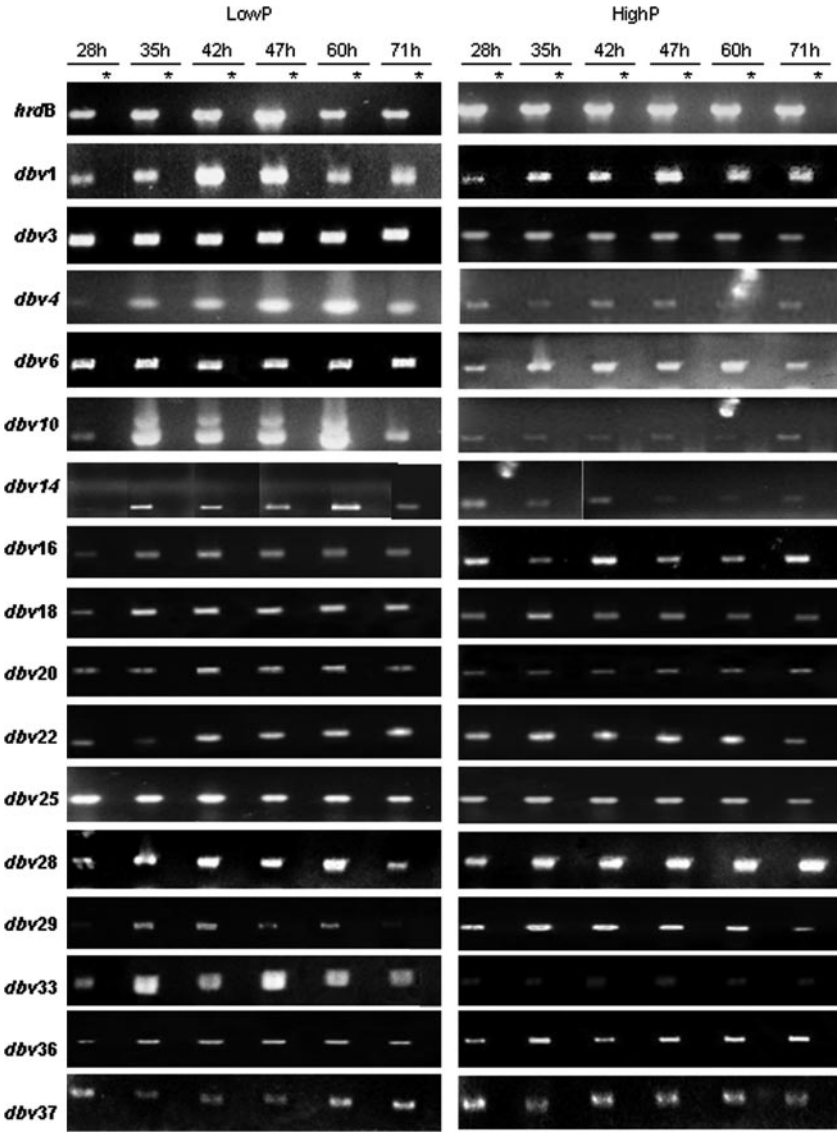

FIG. 3. Transcriptional analysis of selected *dbv* genes under LowP and HighP conditions. RNA samples, extracted from mycelium after 28, 35, 42, 47, 60, and 71 h were analyzed by RT-PCR using primers specific for each *dbv* gene and for *hrdB* (see Table S1 in the supplemental material). Asterisks indicate negative controls (no reverse transcriptase).

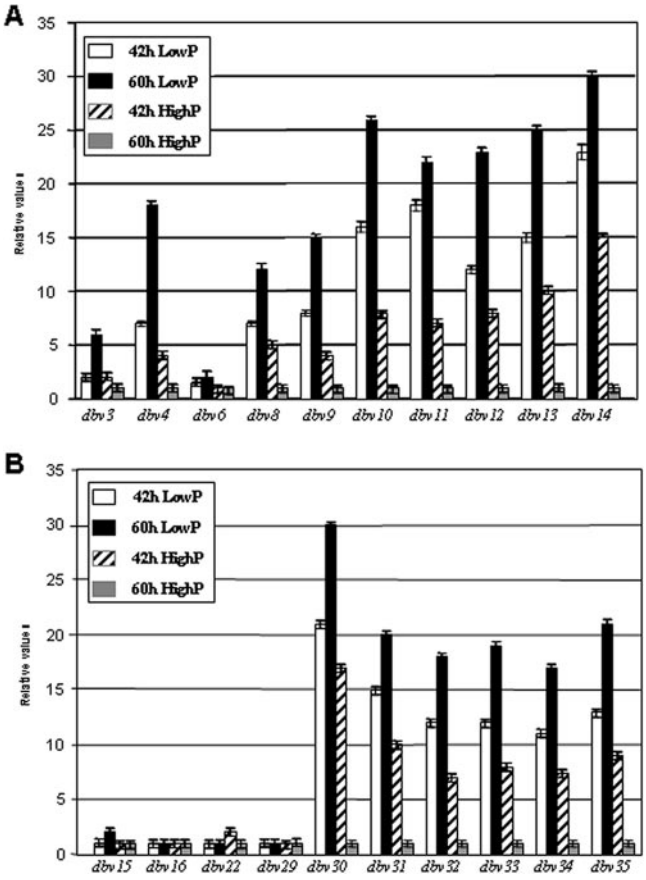

FIG. 4. Real-time RT-PCR analysis of *dbv3*, *dbv4*, *dbv6*, *dbv8*, *dbv9*, *dbv10*, *dbv11*, *dbv12*, *dbv13*, and *dbv14* (A) and *dbv15*, *dbv16*, *dbv22*, *dbv29*, *dbv30*, *dbv31*, *dbv32*, *dbv33*, *dbv34*, and *dbv35* (B) under LowP and HighP conditions. mRNA levels after 42 and 60 h are expressed as relative values to *hrdB*, arbitrarily setting the ratio values for the 60-h, HighP sample to 1. Error bars are calculated from three independent determinations of mRNA abundance in each sample (see Materials and Methods).

Indeed, *dbv4* mRNA levels under LowP were about 2- and 18-fold higher at 42 and 60 h, respectively, than under HighP. In a similar way, all genes within the *dbv14-dbv8* and *dbv30-dbv35* transcripts were more abundant under LowP than HighP conditions (in both cases, about 2-fold and 15- to 30-fold increases at 42 and 60 h, respectively). Moreover, there was a moderate negative effect of phosphate on *dbv3* expression at 60 h, while no variations in *dbv6*, *dbv15*, *dbv16*, *dbv22*, and *dbv29* mRNA levels were observed (Fig. 4). These results indicate that phosphate depletion influences the A40926 production by transcriptional upregulation and that, among the *dbv* genes analyzed, only the regulatory gene *dbv4*, and the biosynthesis genes *dbv14-dbv8* and *dbv30-dbv35* were significantly affected by phosphate.

Identification of the *dbv14* promoter. The finding that *dbv15* and *dbv16* were not influenced by phosphate, while the *dbv14-dbv8* genes were, suggested the presence of a phosphate-controlled promoter upstream of *dbv14* (Fig. 1A). This was confirmed by a promoter probe assay. A 171-bp fragment, containing the upstream region of *dbv14*, was cloned in the promoter probe vector pIJ486. *S. lividans* clones containing the resulting construct showed resistance to 400 μg of kanamycin/ml and to 200 μg of neomycin/ml, while *S. lividans* clones containing the empty vector did not grow in the presence of 50 μg of kanamycin/ml (data not shown).

The transcription start site of *dbv14* was determined by 5′-RACE (rapid amplification of cDNA ends), using total RNA extracted at 47 h under LowP conditions. The sequence of the cloned amplification product started with the first G of the *dbv14* GTG translation initiation codon (Fig. 5A), suggesting that *dbv14* is transcribed as a leaderless mRNA. On the basis of the consensus of streptomycete *E. coli*-like promoters (TTGACPu and TAGPuPuT, 16 to 18 nucleotides apart [39]), the sequences GTGACG, 5 nucleotides upstream of the observed transcription start point, and CACCGT, 16 nucleotides apart, represent the likely −10 and −35 hexamers, respectively, of the *dbv14* promoter (Fig. 5A).

Altogether, these results confirmed the existence of a pro-

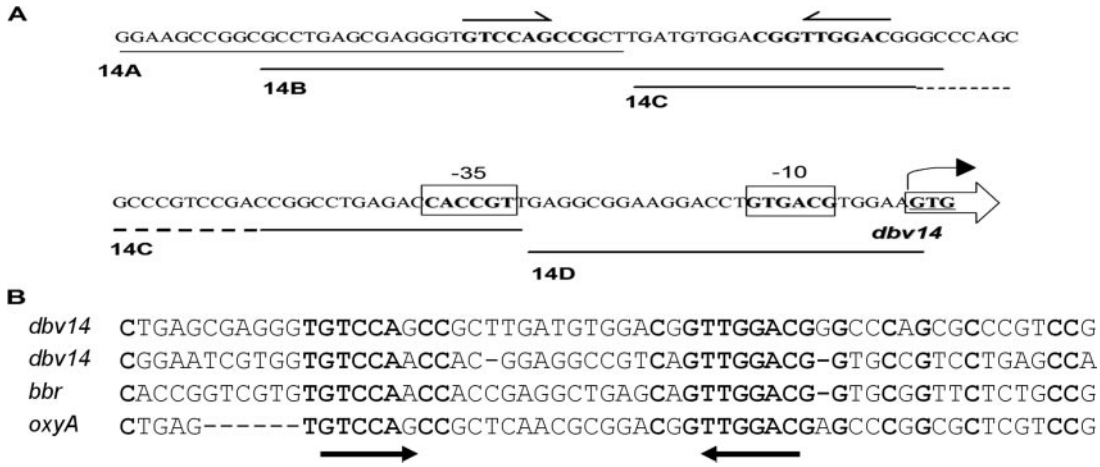

FIG. 5. Identification of the Dbv4 binding site. (A) *dbv14* promoter region. The open arrow represents the *dbv14* gene, the bent arrow represents the most probable transcription start site, and the boxes indicate the deduced −10 and −35 regions. The black arrows indicate the putative Dbv4 binding site. The fragments (14A to 14D) used as electrophoretic mobility shift assay probes are indicated below. (B) Alignment of the StrR-like binding sites. Nucleotides conserved in the four sequences are in boldface. The inverted repeats are indicated by arrows.

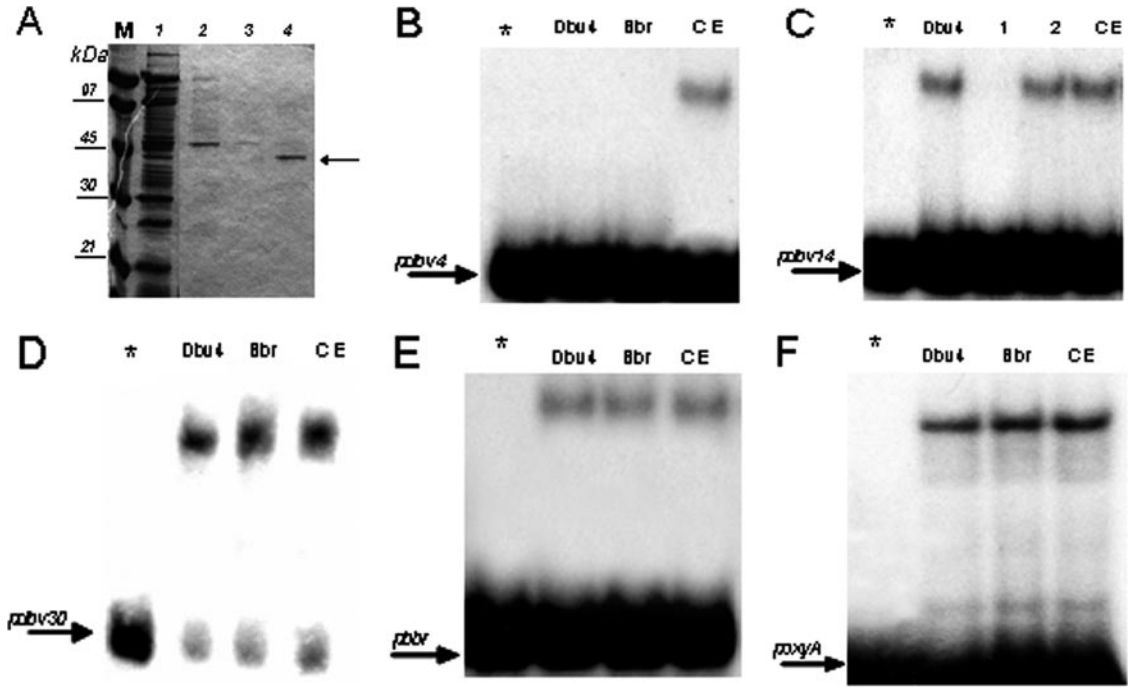

FIG. 6. Purification of His_6-tagged Dbv4 and gel mobility shift assays. (A) SDS-PAGE analysis of His_6-tagged Dbv4 purification. Lane 1, cell extract (25 μg of proteins) from an IPTG-induced culture of *E. coli* BL21(DE3)pLysS containing pRSET-Dbv4. Lanes 2, 3, and 4, pooled Ni-NTA fractions were eluted with 50, 150, and 250 mM imidazole, respectively. The arrow indicates the His_6-tagged Dbv4 protein. Molecular mass standards are indicated on the left. (B to F) Gel mobility shift assays of DNA regions upstream of *dbv4* (B), *dbv14* (C), *dbv30* (D), *bbr* (E), and *oxyA* (F) with Dbv4, Bbr, or *Nonomuraea* total proteins (CE). Lanes labeled with an asterisk contained the probe only. All lanes contained 0.4 ng of ^{32}P-end-labeled target DNA. The binding reactions reported in panel C were carried out in the presence of a 200-fold molar excess of unlabeled probe (lane 1) and a 200-fold molar excess of unlabeled competitor DNA (lane 2).

moter upstream of *dbv14*, which drives enhanced expression of the *dbv14-dbv8* operon under phosphate-limited conditions. Readthrough of this operon from upstream promoter(s) must also occur, since RT-PCR analysis indicated the presence of a transcript spanning *dbv15* and *dbv14* (Fig. 1B).

In vitro binding of His_6-tagged Dbv4 to the *dbv14* and *dbv30* promoters. Dbv4 is 321 amino acids long and shows 45 to 49% identity to StrR, the pathway-specific transcriptional activator of streptomycin biosynthesis in *S. griseus* and *S. glaucescens* (28, 43). Dbv4 contains a putative dimerization domain (residues 14 to 98), homologous to the ParB-like nuclease domain (2), and a putative helix-turn-helix DNA-binding domain (residues 183 to 204). Since, after growth at low levels of phosphate, the *dbv14-dbv8* and *dbv30-dbv35* operons were upregulated similarly to *dbv4*, which encodes a StrR-like regulator, Dbv4 may act as a positive regulator of A40926 biosynthesis by binding at or near the *dbv4*, *dbv14*, and *dbv30* promoters, thereby activating their transcription. In order to verify whether Dbv4 does have DNA-binding activity, Dbv4 was overexpressed in *E. coli* as an N-terminal His_6-tagged protein and purified (Fig. 6A). Gel mobility shift assays of the *dbv4*, *dbv14*, and *dbv30* upstream regions were carried out using purified, His_6-tagged Dbv4.

Dbv4 was clearly unable to bind to its own upstream region, while this DNA segment was upshifted in the presence of *Nonomuraea* total proteins (Fig. 6B). In contrast, Dbv4 was able to bind specifically the upstream regions of *dbv14* and *dbv30*, giving a shift undistinguishable from that observed in the presence of native *Nonomuraea* proteins (Fig. 6C and D). The binding of Dbv4 to the *dbv14* and *dbv30* upstream regions was not affected by excess aspecific competitors (Fig. 6C and data not shown, respectively).

Cross-binding among glycopeptide regulators. A40926 and balhimycin belong to two distinct families of glycopeptides that differ in their heptapeptide skeletons. The *dbv* and *bal* clusters share 25 orthologs out of 37 and 35 genes, respectively. In particular, the *bal* cluster encodes a Dbv4 ortholog, named Bbr, which has recently been shown to specifically bind to the upstream regions of five *bal* genes, including itself (30). Dbv4 and Bbr, which share 80% identity, possess the same predicted helix-turn-helix motif and very similar dimerization domains. Thus, we tested the ability of Bbr to bind to Dbv4-recognized fragments and of Dbv4 to interact with Bbr-bound sequences.

Bbr bound to the *dbv30* upstream region, giving a shift identical to that observed in the presence of Dbv4. The same result was observed with the *dbv14* upstream region (data not shown). As expected, Bbr did not bind to the region upstream of *dbv4* (Fig. 6B). Conversely, Dbv4 bound to two selected regions from the *bal* cluster, the upstream regions of *bbr* (Fig. 6E) and *oxyA*, encoding a P450 monooxygenase (Fig. 6F). Also in this case, Bbr and Dbv4 gave identical band shifts. The binding of Dbv4, Bbr, and native *Nonomuraea* proteins to the *bbr* and *oxyA* upstream regions was not affected by excess aspecific competitors (data not shown).

When the DNA sequences of the upstream regions of *dbv14*, *dbv30*, *bbr*, and *oxyA* were compared, a highly conserved pal-

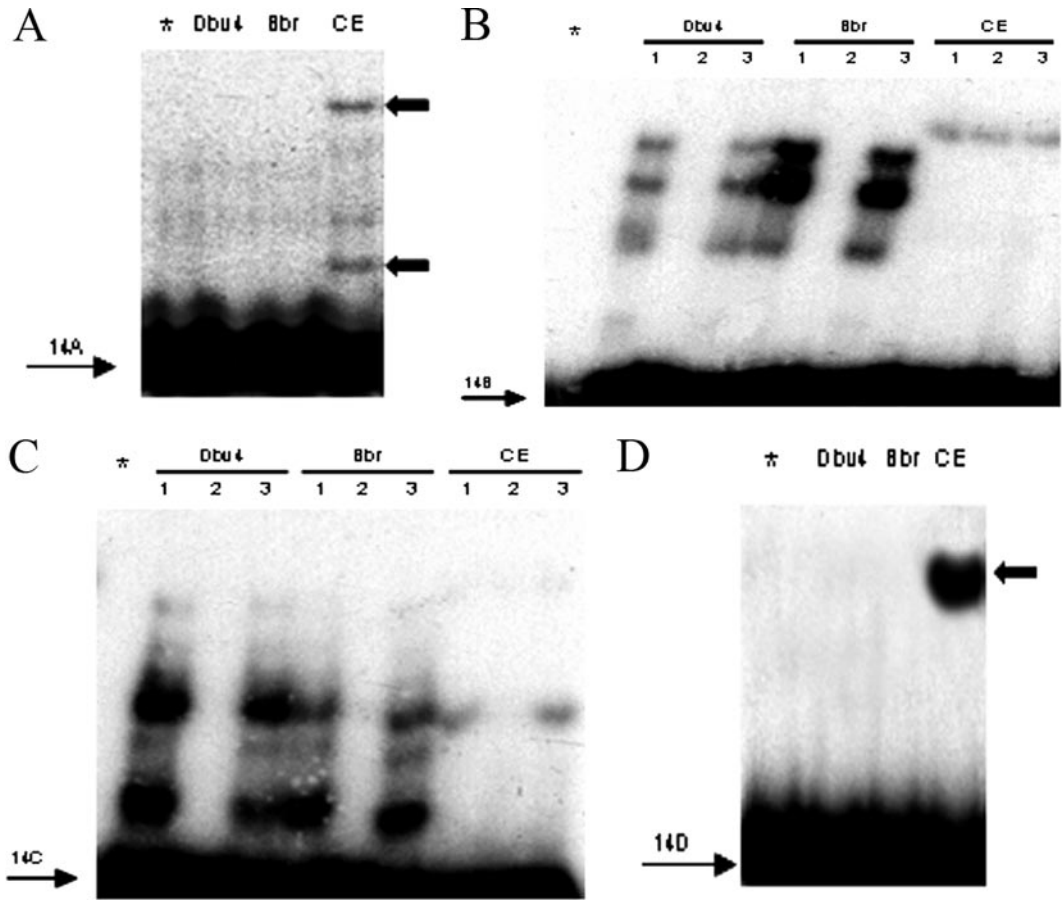

FIG. 7. Gel mobility shift assays of ^{32}P-end-labeled fragments 14A (A), 14B (B), 14C (C), and 14D (D) with Dbv4, Bbr, or *Nonomuraea* total proteins (CE). All samples contained 0.4 ng of labeled target DNA. The asterisks indicate the lane containing the probe only. Lanes: 1, binding reaction; 2, same as in lane 1 but with a 200-fold molar excess of unlabeled probe; 3, same as in lane 1 but with a 200-fold molar excess of unlabeled aspecific competitor DNA added. Arrows denote bands observed with fragments A and D and total *Nonomuraea* proteins.

indrome was found in all fragments, with the consensus sequence GTCCAR$(N)_{17}$TTGGAC (Fig. 5B). This sequence was proposed as the Bbr binding site in the five regions of the *bal* cluster (30) and is part of a conserved intergenic region present in all five clusters devoted to glycopeptide biosynthesis (9).

To further investigate the Dbv4 binding site, four partially overlapping 50-bp DNA fragments (Fig. 5A) were used in gel mobility assays. Fragment 14B contains the entire GTCCAR $(N)_{17}$TTGGAC palindrome, while its 5′ and the 3′ halves are contained within fragments 14A and 14C, respectively. Fragment 14D contains part of the putative −35 region. Dbv4 and Bbr were unable to bind fragments 14A (Fig. 7A) or 14D (Fig. 7D). Unexpectedly, both proteins bound fragments 14B (Fig. 7B) and 14C (Fig. 7C), yielding three and two major complexes, respectively. When incubated with *Nonomuraea* total proteins, fragment 14C was shifted to a position indistinguishable from that of the highest complex observed with Dbv4. However, fragment 14B formed a high-molecular-weight complex with *Nonomuraea* proteins which was not affected by excess unlabeled probe (Fig. 7B). It should be noted that also fragments 14A and 14D were shifted by *Nonomuraea* total proteins (Fig. 7A and D).

These results suggest that conserved palindrome GTCCAR $(N)_{17}$TTGGAC actually does correspond to an in vitro binding site for Dbv4 and Bbr. However, the ability of these proteins to equally bind to fragment 14C suggests that either a partial palindrome is sufficient for binding or that other features present within this fragment are responsible for the interaction.

DISCUSSION

The present study provides experimental evidence for the function of Dbv4 as a DNA-binding protein which acts as a positive regulator of A40926 biosynthesis by controlling expression of two operons of the *dbv* cluster: the *dbv14-dbv8* operon, encoding the four cross-linking oxygenases, the halogenase, the *N*-acetylglucosamine transferase and the *N*-acylase, and the *dbv30-dbv35* operon, encoding the four enzymes involved in DPG biosynthesis (5, 25), as well as the sodium-proton antiporter and a protein of unknown function. In the present study, we demonstrate that the expression of *dbv4* and of the *dbv14-dbv8* and *dbv30-dbv35* operons is negatively influenced by phosphate by RT-PCR analysis and real-time RT-

PCR experiments (Fig. 3 and 4) and that in vitro Dbv4 binds to the region upstream of *dbv14* and *dbv30* (Fig. 6).

In vitro, Dbv4 and its ortholog Bbr were found to equally bind four distinct regions: the 171-bp fragment containing the *dbv14* promoter (Fig. 6C), the 351-bp fragment upstream to *dbv30* (Fig. 6D), the 158-bp segment containing the *bbr* promoter (Fig. 6E) and the 232-bp fragment containing the *oxyA* promoter (Fig. 6F). In addition, the mobility shifts observed with Dbv4, Bbr, or *Nonomuraea* total proteins were indistinguishable (Fig. 6C to F). The four regions share the palindrome GTCCAR$(N)_{17}$TTGGAC, proposed as the Bbr binding site (30) and similar to the experimentally determined StrR binding site GTTCRACTG-$(N)_{11}$-CRGTYGAAC (28). This palindrome is located 28 nucleotides upstream of the −35 promoter sequence of *dbv14*, suggesting a direct interaction between Dbv4 and RNA polymerase (23).

When 50-bp fragments were used in mobility shift assays, two or three retarded complexes were observed (Fig. 7B and C). These results are consistent with the presence in Dbv4 of a dimerization domain and suggest that Dbv4 in vitro can bind DNA as a monomer, dimer, or tetramer, as reported for ParB (2). Since a single band was observed using the 171-bp fragment (Fig. 6B), Dbv4 might bind as a tetramer to this fragment. With smaller fragments, binding by Dbv4 might not be as effective, resulting in the formation of different complexes. Further experiments are necessary to corroborate this hypothesis and to establish whether binding of Dbv4 to fragment 14C has any biological relevance.

Our results suggest that Dbv4, by interacting with the regions upstream of the *dbv30-dbv35* and *dbv14-dbv8* operons, controls expression of these genes. We have not attempted to knockout *dbv4* in *Nonomuraea*, since genetic manipulation in this strain is not efficient (38) and repeated attempts at inactivating *bbr* in the balhimycin producer *Amycolatopsis balhimycina* have thus far failed (E. Stegmann, unpublished data).

The *dbv* cluster appears to contain just two binding sites for Dbv4, while the *bal* cluster contains five Bbr binding sites (30). Judging from the presence of conserved intergenic regions, the *cep*, *sta*, and *tcp* clusters should contain at least two, one, and four predicted Dbv4-binding palindromes, respectively (9). In all five clusters, one putative binding site is located 5′ to *oxyA* orthologs. This gene encodes the P450 monooxygenase responsible for cross-linking amino acids 2 and 4 (3). The Oxy enzymes catalyze a critical step, probably the most distinctive feature in glycopeptide biosynthesis. Current evidence indicates that at least some of the Oxy enzymes act in concert with the NRPS while the growing peptide is still enzyme bound (3, 36, 46). In all glycopeptide clusters characterized to date, the *oxy* genes are linked and an *oxyA* ortholog is always the first gene, suggesting the existence of an operon in all cases. Since all glycopeptide clusters encode an StrR-like regulator, it is tempting to speculate that expression of the *oxy* genes is controlled in all clusters by the same regulator. Consistently, we observed that Bbr is able to bind to *dbv* sequences and, vice versa, that Dbv4 recognizes at least some *bal* sequences. This conservation of a regulatory circuit is quite remarkable, considering that these clusters are quite divergent and derive from four different genera (*Actinoplanes*, *Amycolatopsis*, *Nonomuraea*, and *Streptomyces*) belonging to an equivalent number of *Actinomycetales* suborders. Cross-binding is thought to have played an essential role in the formation of new regulatory pathways during evolution, which allowed primitive regulation of horizontally acquired genes (8).

Apart from the common regulation of the *oxy*-genes via a Dbv4-type regulator (Fig. 6C to F), different regulatory strategies are apparently adopted in the other clusters. Indeed, Dbv4 controls also the *dbv30-dbv35* operon (Fig. 6D), involved in DPG biosynthesis. A Dbv4-type palindrome is also present upstream of the *dbv31* ortholog in the *tcp* cluster (9), suggesting a similar type of regulation. In contrast, Bbr controls its own expression (30), and probably the same occurs in the chloroeremomycin case, while we have shown that no binding occurs between Dbv4 and its upstream region (Fig. 6B). Similarly, the StrR-like regulator is not expected to control its own expression in the *sta* and *tcp* clusters.

According to the data presented here, we can suggest that phosphate depletion induces *dbv4* transcription, which allows Dbv4 to bind to the *dbv14* and *dbv30* promoters and enhance expression of the corresponding operons. The expression of most analyzed *dbv* genes was not influenced by phosphate, but we cannot rule out phosphate effects at the posttranslational level or on the enzymatic activity.

The biosynthesis of many different antibiotics and secondary metabolites is regulated by phosphate (17, 19, 20). At least for candicidin in *S. griseus*, oxytetracycline in *S. rimosus*, and pimaricin in *S. natalensis*, phosphate control is exerted at the transcriptional level (1, 21, 22). Recently, insights into the molecular mechanisms through which phosphate controls global antibiotic production have started to emerge: phosphate control of antibiotic biosynthesis in *Streptomyces coelicolor* and *S. lividans* is mediated by the two-component system PhoR-PhoP (31), with PhoP binding to promoters of phosphate-regulated genes in *S. coelicolor* (32). Moreover, another gene (*ppk*) related to phosphate metabolism, was shown to play a key role in the regulation of antibiotic biosynthesis in *S. lividans* (7) pointing out the role of the polyphosphate stores in the regulation of antibiotic biosynthesis in *Actinomycetes*. However, we did not identify Pho boxes (as defined by reference 32) in the *dbv4* upstream region, and it remains to be determined whether *Nonomuraea* contains *phoR*/*phoP* orthologs.

To our knowledge, this is the first report describing the molecular mechanism of phosphate effects on glycopeptide production, and it suggests that mechanisms similar to those described in *Streptomyces* spp. operate also in less-studied actinomycete genera such as *Nonomuraea*. As observed for other antibiotic pathways, one may expect that other nutrients, stress factors, and cell-to-cell signals (41) may contribute to the transcriptional control of the *dbv* cluster. *dbv3* and *dbv4* contain one and three TTA codons, respectively, so their expression might be dependent on *bldA*, the structural gene for $tRNA^{UUA}$ (16), if this mechanism operates in *Nonomuraea* as well. It remains to be determined whether the other regulators encoded by the *dbv* cluster affect *dbv4* expression or if its enhanced mRNA levels under LowP conditions are due to the absence of a repressor. Detailed studies of the mechanisms of *dbv4* transcriptional activation, as well as investigation of the effects of other signals, will further elucidate the regulation of glycopeptide production and enable rational approaches to-

ward the generation of overproducers of the dalbavancin precursor.

ACKNOWLEDGMENTS

This study was supported by the European Union via COMBIGTOP project LSHB-CT-2003-503491.

We acknowledge our coworkers participating in these projects for stimulating discussions and especially Evi Stegmann, Riham Shawky, and Wolfgang Wohlleben for support. We thank Margherita Sosio for helpful suggestions and Rosa Passantino for technical advice.

This study is dedicated to the memory of Benedetta Catalano.

REFERENCES

1. **Asturias, J. A., P. Liras, and J. F. Martin.** 1990. Phosphate control of *pabS* gene transcription during candicidin biosynthesis. Gene **93:**79–84.
2. **Bartosik, A. A., K. Lasocki, J. Mierzejewska, C. M. Thomas, and G. Jagura-Burdzy.** 2004. ParB of *Pseudomonas aeruginosa*: interactions with its partner ParA and its target *parS* and specific effects on bacterial growth. J. Bacteriol. **186:**6983–6998.
3. **Bischoff, D., B. Bister, M. Bertazzo, V. Pfeifer, E. Stegmann, G. J. Nicholson, S. Keller, S. Pelzer, W. Wohlleben, and R. D. Sussmuth.** 2005. The biosynthesis of vancomycin-type glycopeptide antibiotics: a model for oxidative side chain cross-linking by oxygenases coupled to the action of peptide synthetases. Chembiochem **6:**267–272.
4. **Candiani, G., M. Abbondi, M. Borgonovi, G. Romano, and F. Parenti.** 1999. *In-vitro* and *in-vivo* antibacterial activity of BI 397, a new semi-synthetic glycopeptide antibiotic. J. Antimicrob. Chemother. **44:**179–192.
5. **Chen, H., C. C. Tseng, B. K. Hubbard, and C. T. Walsh.** 2001. Glycopeptide antibiotic biosynthesis: enzymatic assembly of the dedicated amino acid monomer (*S*)-3,5-dihydroxyphenylglycine. Proc. Natl. Acad. Sci. USA **98:** 14901–14906.
6. **Chiu, H. T., B. K. Hubbard, A. N. Shah, J. Eide, R. A. Fredenburg, C. T. Walsh, and C. Khosla.** 2001. Molecular cloning and sequence analysis of the complestatin biosynthetic gene cluster. Proc. Natl. Acad. Sci. USA **98:**8548–8553.
7. **Chouayekh, H., and M. J. Virolle.** 2002. The polyphosphate kinase plays a negative role in the control of antibiotic production in *Streptomyces lividans*. Mol. Microbiol. **43:**919–930.
8. **de Lorenzo, V., and J. Perez-Martin.** 1996. Regulatory noise in prokaryotic promoters: how bacteria learn to respond to novel environmental signals. Mol. Microbiol. **19:**177–1184.
9. **Donadio, S., M. Sosio, E. Stegmann, T. Weber, and W. Wohlleben.** 2005. Comparative analysis and insights into the evolution of gene clusters for glycopeptide antibiotic biosynthesis. Mol. Genet. Genomics **274:**40–50.
10. **Eustáquio, A. S., S. M. Li, and L. Heide.** 2005. NovG, a DNA-binding protein acting as a positive regulator of novobiocin biosynthesis. Microbiology **151:** 1949–1961.
11. **Goldstein, B. P., E. Selva, L. Gastaldo, M. Berti, R. Pallanza, F. Ripamonti, P. Ferrari, M. Denaro, V. Arioli, and G. Cassani.** 1987. A40926, a new glycopeptide antibiotic with anti-*Neisseria* activity. Antimicrob. Agents Chemother. **31:**1961–1966.
12. **Gunnarsson, N., P. Bruheim, and J. Nielsen.** 2003. Production of the glycopeptide antibiotic A40926 by *Nonomuraea* sp. ATCC 39727: influence of medium composition in batch fermentation. J. Ind. Microbiol. Biotechnol. **30:**150–156.
13. **Ikeno, S., D. Aoki, K. Sato, M. Hamada, M. Hori, and K. S. Tsuchiya.** 2002. *kasT* gene of *Streptomyces kasugaensis* M338–M1 encodes a DNA-binding protein which binds to intergenic region of *kasU-kasJ* in the kasugamycin biosynthesis gene cluster. J. Antibiot. **55:**1053–1062.
14. **Kahne, D., C. Leimkuhler, W. Lu, and C. Walsh.** 2005. Glycopeptide and lipoglycopeptide antibiotics. Chem. Rev. **105:**425–448.
15. **Kieser, T., M. J. Bibb, M. J. Buttner, K. F. Chater, and D. A. Hopwood.** 2000. Practical *Streptomyces* genetics. John Innes Foundation, Norwich, United Kingdom.
16. **Leskiw, B. K., E. J. Lawlor, J. M. Fernandez-Abalos, and K. F. Chater.** 1991. TTA codons in some genes prevent their expression in a class of developmental, antibiotic-negative, *Streptomyces* mutants. Proc. Natl. Acad. Sci. USA **88:**2461–2465.
17. **Liras, P., J. A. Asturias, and J. F. Martin.** 1990. Phosphate control sequences involved in transcriptional regulation of antibiotic biosynthesis. Trends Biotechnol. **8:**184–189.
18. **Li, T. L., F. Huang, S. F. Haydock, T. Mironenko, P. F. Leadlay, and J. B. Spencer.** 2004. Biosynthetic gene cluster of the glycopeptide antibiotic teicoplanin: characterization of two glycosyltransferases and the key acyltransferase. Chem. Biol. **11:**107–119.
19. **Martín, J. F.** 1989. Molecular mechanism for the control by phosphate of the biosynthesis of antibiotic and secondary metabolites, p. 213–237. *In* S. Shapiro (ed.), Regulation of secondary metabolism in actinomycetes. CRC Press, Inc., Boca Raton, FL.
20. **Masuma, R., Y. Tanaka, H. Tanaka, and S. Omura.** 1986. Production of nanaomycin and other antibiotics by phosphate-depressed fermentation using phosphate-trapping agents. J. Antibiot. **39:**1557–1564.
21. **McDowall, K. J., A. Thamchaipenet, and I. S. Hunter.** 1999. Phosphate control of oxytetracycline production by *Streptomyces rimosus* is at the level of transcription from promoters overlapped by tandem repeats similar to those of the DNA-binding sites of the OmpR family. J. Bacteriol. **181:**3025–3032.
22. **Mendes, M. V., S. Tunca, N. Anton, E. Recio, A. Sola-Landa, J. F. Aparicio, and J. F. Martin.** 2007. The two-component *phoR-phoP* system of *Streptomyces natalensis*: inactivation or deletion of *phoP* reduces the negative phosphate regulation of pimaricin biosynthesis. Metab. Eng. **9:**217–227.
23. **Ohnishi, Y., H. Yamazaki, J. Kato, A. Tomono, and S. Horinouchi.** 2005. Adpa, a central transcriptional regulator in the A-factor regulatory cascade that leads to morphological development and secondary metabolism in *Streptomyces griseus*. Biosci. Biotechnol. Biochem. **69:**431–439.
24. **Pelzer, S., R. Sussmuth, D. Heckmann, J. Recktenwald, P. Huber, G. Jung, and W. Wohlleben.** 1999. Identification and analysis of the balhimycin biosynthetic gene cluster and its use for manipulating glycopeptide biosynthesis in *Amycolatopsis mediterranei* DSM5908. Antimicrob. Agents Chemother. **43:**1565–1573.
25. **Pfeifer, V., G. J. Nicholson, J. Ries, J. Recktenwald, A. B. Schefer, R. M. Shawky, J. Schroder, W. Wohlleben, and S. Pelzer.** 2001. A polyketide synthase in glycopeptide biosynthesis: the biosynthesis of the non-proteinogenic amino acid (*S*)-3,5-dihydroxyphenylglycine. J. Biol. Chem. **276:**38370–38377.
26. **Pootoolal, J., M. G. Thomas, C. G. Marshal, J. M. Neu, B. K. Hubbard, C. T. Walsh, and G. D. Wright.** 2002. Assembling the glycopeptide antibiotic scaffold: the biosynthesis of A47934 from *Streptomyces toyocaensis* NRRL15009. Proc. Natl. Acad. Sci. USA **99:**8962–8967.
27. **Recktenwald, J., R. Shawky, O. Puk, F. Pfennig, U. Keller, W. Wohlleben, and S. Pelzer.** 2002. Nonribosomal biosynthesis of vancomycin-type antibiotics: a heptapeptide backbone and eight peptide synthetase modules. Microbiology **148:**1105–1118.
28. **Retzlaff, L., and J. Distler.** 1995. The regulator of streptomycin gene expression, StrR, of *Streptomyces griseus* is a DNA binding activator protein with multiple recognition sites. Mol. Microbiol. **18:**151–162.
29. **Sambrook, J., E. F. Fritsch, and T. Maniatis.** 1982. Molecular cloning: a laboratory manual. Cold Spring Harbor Laboratory, New York, NY.
30. **Shawky, R. M., O. Puk, A. Wietzorrek, S. Pelzer, E. Takano, W. Wohlleben, and E. Stegmann.** 2007. The border sequence of the balhimycin biosynthesis gene cluster from *Amycolatopsis balhimycina* contains *bbr*, encoding a StrR-like pathway-specific regulator. J. Mol. Microb. Biotech. **13:**76–88.
31. **Sola-Landa, A., R. S. Moura, and J. F. Martin.** 2003. The two-component PhoR-PhoP system controls both primary metabolism and secondary metabolite biosynthesis in *Streptomyces lividans*. Proc. Natl. Acad. Sci. USA **100:** 6133–6138.
32. **Sola-Landa, A., A. Rodriguez-Garcia, E. Franco-Dominguez, and J. F. Martin.** 2005. Binding of PhoP to promoters of phosphate-regulated genes in *Streptomyces coelicolor*: identification of PHO boxes. Mol. Microbiol. **56:** 1373–1385.
33. **Sosio, M., S. Stinchi, F. Beltrametti, A. Lazzarini, and S. Donadio.** 2003. The gene cluster for the biosynthesis of the glycopeptide antibiotic A40926 by *Nonomuraea* sp. Chem. Biol. **10:**541–549.
34. **Sosio, M., H. Kloosterman, A. Bianchi, P. de Vreugd, L. Dijkhuizen, and S. Donadio.** 2004. Organization of the teicoplanin gene cluster in *Actinoplanes teichomyceticus*. Microbiology **150:**95–102.
35. **Sosio, M., and S. Donadio.** 2006. Understanding and manipulating glycopeptide pathways: the example of the dalbavancin precursor A40926. J. Ind. Microbiol. Biotechnol. **33:**569–576.
36. **Stegmann, E., S. Pelzer, D. Bischoff, O. Puk, S. Stockert, D. Butz, K. Zerbe, J. Robinson, R. D. Sussmuth, and W. Wohlleben.** 2006. Genetic analysis of the balhimycin (vancomycin-type) oxygenase genes. J. Biotechnol. **5:**640–653.
37. **Steiert, M., and F. J. Schmitz.** 2002. Dalbavancin (Biosearch Italia/Versicor). Curr. Opin. Investig. Drugs **3:**229–233.
38. **Stinchi, S., S. Azimonti, S. Donadio, and M. Sosio.** 2003. A gene transfer system for the glycopeptide producer *Nonomuraea* sp. ATCC 39727. FEMS Microbiol. Lett. **225:**53–57.
39. **Strohl, W. R.** 1992. Compilation and analysis of DNA sequences associated with apparent streptomycete promoters. Nucleic Acids Res. **20:**961–974.
40. **Sussmuth, R. D., and W. Wohlleben.** 2004. The biosynthesis of glycopeptide antibiotics-a model for complex, non-ribosomally synthesized, peptidic secondary metabolites. Appl. Microbiol. Biotechnol. **63:**344–350.
41. **Takano, E.** 2006. Gamma-butyrolactones: *Streptomyces* signalling molecules regulating antibiotic production and differentiation. Curr. Opin. Microbiol. **9:**287–294.
42. **Technikova-Dobrova, Z., F. Damiano, S. M. Tredici, G. Vigliotta, R. Di**

Summa, L. Palese, A. Abbrescia, N. Labonia, G. V. Gnoni, and P. Alifano. 2004. Design of mineral medium for growth of *Actinomadura* sp. ATCC 39727, producer of the glycopeptide A40926: effects of calcium ions and nitrogen sources. Appl. Microbiol. Biotechnol. **65:**671–677.

43. **Thamm, S., and J. Distler.** 1997. Properties of C-terminal truncated derivatives of the activator, StrR, of the streptomycin biosynthesis in *Streptomyces griseus*. FEMS Microbiol. Lett. **149:**265–272.
44. **Van Wageningen, A. M., P. N. Kirkpatrick, D. H. Williams, B. R. Harris, J. K. Kershaw, N. J. Lennard, M. Jones, S. J. Jones, and P. J. Solenberg.** 1998. Sequencing and analysis of genes involved in the biosynthesis of a vancomycin group antibiotic. Chem. Biol. **5:**155–162.
45. **Williams, D. H., and B. Bardsley.** 1999. The vancomycin group of antibiotics and the fight against resistant bacteria. Angew. Chem. Int. **38:** 1172–1193.
46. **Zerbe, K., K. Woithe, D. B. Li, F. Vitali, L. Bigler, and J. A. Robinson.** 2004. An oxidative phenol coupling reaction catalyzed by *oxyB*, a cytochrome P450 from the vancomycin-producing microorganism. Angew. Chem. Int. **43:** 6709–6713.